The Environment of [2Fe-2S] Clusters in Ferredoxins: The Role of Residue 45 Probed by Site-Directed Mutagenesis†

Momcilo Vidakovic, Grazyna Fraczkiewicz, Bakul C. Dave, Roman S. Czernuszewicz, and Juris P. Germanas*

Department of Chemistry, University of Houston, Houston, Texas 77204-5641

Received June 5, 1995; Revised Manuscript Received August 22, 1995⊗

ABSTRACT: The biochemical and biophysical properties of the Ala45Ser mutant of the [2Fe-2S] ferredoxin from vegetative cells of the cyanobacterium *Anabaena* sp. 7120 are described. This novel protein, which incorporates the residue present in many higher plant ferredoxins into the analogous position of a typical cyanobacterial ferredoxin, was prepared to probe the origin of the characteristic spectrochemical and functional differences between the ferredoxins from these two sources. The variant protein was produced by site-directed mutagenesis and was expressed as the holoprotein in *Escherichia coli*. Although the UV−vis spectrum of the Ala45Ser mutant was indistinguishable from that of the wild-type (WT) protein, the circular dichroism (CD) spectrum of the mutant was distinct and similar in appearance to that of spinach ferredoxin, which possesses a Ser residue at the analogous position. The values of the principal *g* factors of the EPR spectrum of the dithionite-reduced mutant protein differed from those of the WT spectrum and resembled those of plant ferredoxins containing serine at position 45. Analysis of the mutant EPR spectrum according to the method of Blumberg indicated greater covalent interactions between the localized ferrous site of the cluster and the protein matrix relative to the WT protein. The resonance Raman spectrum of Ala45Ser *Anabaena* ferredoxin was distinct from the spectrum of the WT protein and showed exceptional similarity to the spectrum of higher plant ferredoxins, such as spinach ferredoxin. The mutant protein spectrum displayed considerably greater deuterium dependent isotope shifts for bands ascribed to terminal Fe−S stretching modes than did the WT spectrum. The larger shifts were attributed to a greater degree of hydrogen bonding between the protein matrix and the ligand cysteinyl sulfur atoms in the Ala45Ser variant than in the WT protein. The midpoint redox potential of Ala45Ser *Anabaena* ferredoxin (−382 mV vs NHE) was notably higher than that of the WT protein (−406 mV) but not in line with those of plant ferredoxins, such as the spinach protein (−420 mV). Altogether, the spectrochemical differences between the WT and Ala45Ser *Anabaena* ferredoxins were ascribed to the presence of an additional hydrogen bond from the side chain hydroxyl group of serine 45 to the sulfur atom of Cys 41 in the mutant protein. The distinction between the spectroscopic properties of the Ala45Ser and the WT *Anabana* ferredoxins and the similarities of the spectral features of the mutant to those of higher plant ferredoxins demonstrate that the identity of the residue at position 45 tunes the microenvironment of the iron−sulfur cluster and primarily dictates the spectrochemical properties of these important proteins.

The [2Fe-2S] ferrdoxins are small iron−sulfur proteins that are widely distributed in nature, where they function as mediators of electron transfer in photosynthesis, substrate hydroxylation, and metabolism (Lovenberg, 1973). These polypeptides incorporate a prosthetic group consisting of a pair of iron atoms, each bound to the thiol functionalities of two cysteine residues, bridged by two sulfide ions. The most extensively investigated class of [2Fe-2S] ferredoxins are the photosynthetic ferredoxins from plant chloroplasts and cyanobacteria, whose primary function is promoting electron transfer between reduced photosystem I and the enzyme ferredoxin−$NADP^+$ reductase (FNR)[1] (Knaff & Hirasawa, 1991). In certain organisms, ferredoxin also functions as an electron carrier in diverse processes such as nitrogen fixation, sulfate and nitrate reduction, and glutamate synthesis (Knaff & Hirasawa, 1991).

The photosynthetic ferredoxins are low-molecular weight proteins (93−98 amino acids) containing a single [2Fe-2S] cluster bound to four cysteine residues (Cys 41, 46, 49, and 79 for *Anabaena* species strain PCC7120 ferredoxin). The amino acid sequences of ferredoxins from over 75 species of cyanobacteria and higher plants have been deduced, and all show considerable homology, including 18 totally invariant positions (Matsubara & Hase, 1983; Matsubara & Saeki, 1992). The crystal structures of four ferredoxins from cyanobacteria [*Spirulina platensis* (Fukuyama et al., 1980, 1981), *Aphanothece sacrum* (Tsukihara et al., 1990), and vegetative (Rypniewski et al., 1991) and heterocyst (Jacobsen et al., 1993) isoforms of *Anabaena* species strain PCC7120] have been determined, revealing that all four polypeptides display identical folds.

† This research was supported by the National Institutes of General Medical Sciences (Grant GM913498 to R.S.C.), the University of Houston, and American Cyanamid (Faculty Research Award to J.P.G.).

* Author to whom correspondence should be addressed.

⊗ Abstract published in *Advance ACS Abstracts,* October 1, 1995.

[1] Abbreviations: CD, circular dichroism; CT, charge transfer; DPV, differential pulse voltammetry; EPR, electron paramagnetic resonance; ET, electron transfer; FNR, ferredoxin−$NADP^+$ reductase; FPLC, fast protein liquid chromatography; HIPIP, high-potential iron protein; IPTG, isopropyl β-thiogalactoside; NHE, normal hydrogen electrode; PCR, polymerase chain reaction; RT, room temperature; Tris, tris(hydroxymethyl)aminomethane; RR, resonance Raman; WT, wild type.

0006-2960/95/0434-13906$09.00/0

Despite the high degree of homology among the photosynthetic ferredoxins, sequence variations result in a considerable degree of physical and functional difference for these proteins. Differences in the spectrochemical and functional properties are particularly noticeable for ferredoxins isolated from higher plants or from cyanobacteria. For example, variations in band intensities and energies in the circular dichroism (CD) and resonance Raman (RR) spectra and in the values of the principal g factors of the electron paramagnetic resonance (EPR) spectra of proteins from plant or cyanobacterial sources are clearly evident. Additionally, the redox potentials of plant ferredoxins are generally lower [−390 to −425 mV vs normal hydrogen electrode (NHE)] than those of cyanobacterial ferredoxins (−310 to −380 vs NHE) (Cammack et al., 1977). Furthermore, functional differences between ferredoxins from the two sources are evident. For instance, reduced plant ferredoxins are more reactive to oxidation by inorganic complexes such as $Co(NH_3)_6^{3+}$ than those from the blue-green algae. These spectroscopic and functional differences are the result of variations in the microenvironment of the [2Fe-2S] cluster, which alter the electronic structure of the metal cluster. The environmental differences originate from sequence variations at select positions between proteins from the two sources, such as insertions, deletions, and the presence of unique amino acids (Matsubara & Saeki, 1992).

To probe the origin of the differences in biophysical properties of different [2Fe-2S] ferredoxins, we are using site-directed mutagenesis to engineer the active sites of these molecules and various spectrochemical and structural techniques to characterize the resultant proteins. The model protein to be used in these studies is the vegetative isoform of the ferredoxin from the cyanobacterium *Anabaena* PCC7120. This protein was chosen due to the availability of a high-resolution crystal structure (Rypniewski et al., 1991) and extensive biophysical characterization (Bohme & Schrautemeier, 1987a; Oh & Markley, 1990; Oh et al., 1990). In this paper, we describe the spectroscopic and electrochemical properties of a novel mutant of *Anabaena* ferredoxin in which residue 45, located on the metal-binding loop in close proximity to the reducible iron atom, is changed from alanine to serine. This mutant was prepared because an alanine residue is found at this position in most cyanobacterial ferredoxins (Rogers, 1987), while a serine is present in most higher plant proteins (Matsubara & Hase, 1983). We present evidence that the identity of the residue at position 45 determines many of the spectroscopic properties of the protein and that the residue plays an important role in modulation of the redox and electron transfer characteristics of the cluster.

EXPERIMENTAL PROCEDURES

Expression of Recombinant Proteins. The previously described clone pAn662 (Alam et al., 1986), containing the entire coding region for vegetative *Anabaena* PCC7120 ferredoxin I gene (*petF*), was used as the template in a polymerase chain reaction (PCR). Synthetic oligonucleotides, 5′-GCGCCATATGGCAACCTTTAAAGTTACA-3′, and 5′-CGCGAGATCTTTAGTAGAGGTCTTCTTCTTT-3′, incorporating *Nde*I and *Bgl*II sites at the 5′ and 3′ ends of the gene, respectively, were used as primers. The amplification product was cloned directly into the *Hinc*II site of the plasmid pTZ18u (Stratagene). The recombinant plasmid pTZ18uAnFd was then digested with *Bgl*II and *Nde*I, and the resulting *petF* fragment was isolated and inserted into the pET-3a expression vector (Novagen), resulting in the plasmid pET-3aAnFd. All plasmid constructs were characterized by restriction analysis.

The *Escherichia coli* strain HMS 174(DE3), which contains a chromosomal copy of the T7 RNA polymerase gene under control of the *lac* promoter, was transformed with pET-3aAnFd. The culture was grown in LB medium supplemented with 100 mg of ampicillin per liter, followed by IPTG (0.3 mM) induction of ferredoxin expression when the culture had reached log phase ($OD_{600} = 0.8$). After cell collection by centrifugation and disruption using a French press, purification of the crude protein was achieved through anion-exchange chromatography on a Q-Sepharose column using a NaCl gradient (0−1 M NaCl) followed by FPLC gel filtration (Superdex 75) and further FPLC anion-exchange chromatography (Mono-Q, 0−0.4 M NaCl). The target protein was isolated in greater than 95% purity by polyacrylamide gel electrophoresis (PAGE) and isoelectric focusing (IEF) using a Phastsystem apparatus. Native PAGE (12%) was preferred, since denaturation of this ferredoxin with sodium dodecyl sulfate (SDS) gave rise to a series of diffuse bands with an apparent molecular mass between 23 and 27 kDa. Spinach ferredoxin was prepared according to the method of Golbeck (Mino et al., 1987). Growth and isolation of ferredoxin from *Anabaena* sp. 7120 was carried out as described (Oh & Markley, 1990).

Site-Directed Mutagenesis. Site-directed mutagenesis was carried out following the Kunkel protocol (Kunkel et al., 1987) using the Muta-Gene Kit from Bio-Rad. Recombinant plasmid pTZ18uAnFd was introduced into competent *E. coli* strain CJ236 (*dut*$^-$, *ung*$^-$). These cells were superinfected with the helper phage M13K07, and single-stranded, uracil-containing DNA carrying the coding strand for *Anabaena* ferredoxin was isolated. The oligonucleotide 5′-TGAG-CATGAACCAGCCCG-3′, which codes for the Ala45Ser mutation, was hybridized to the single-stranded copy of pTZ18uAnFd. The complementary strand was then synthesized and ligated. The double-stranded target vector, completely homologous except for the intended mutation, was transformed into competent *E. coli* strain MV 1190. The mutated recombinant vector, pTZ18uAnFdA45S, was identified by the Sanger dideoxy chain-termination sequencing method (Maniatis et al., 1989). Subcloning of the mutant plasmid into the pET-3a expression vector was carried out as described for the wild type (WT).

Spectroscopic Characterization. The UV−vis spectra of the proteins in 20 mM Tris-HCl buffer, pH 7.5, at room temperature (RT) were obtained using an HP 8452A Diode Array spectrophotometer. CD spectra of ferredoxins in 20 mM sodium phosphate buffer, pH 7.4, at RT were recorded on a Jasco J-700 spectropolarimeter. The EPR spectra of 1 mM dithionite-reduced ferredoxins in 20 mM Tris-HCl, pH 8.0, were obtained using a Bruker ESP-300 apparatus, interfaced with an Oxford Instruments ESR-900 liquid helium continuous flow cryostat at 10 K. Modulation amplitudes were 4 G at 1 mW power, and spectral frequencies were 9.799 or 9.72 GHz. Simulations of the spectra were carried out using the EPR program written by Frank Neese (Quan-

tum Chemistry Program Exchange, Bloomington, IN 47405, Program QCMP136).

The resonance Raman spectra of the ferredoxins in 20 mM Tris-HCl at 77 K were obtained by excitation with the 457.9, 488, or 514.5 nm line from a coherent 90-6 Ar^+ ion laser using the Raman instrumentation described elsewhere (Czernuszewicz, 1993). Samples in D_2O were prepared as follows. A 0.5 mL sample in 20 mM Tris-HCl was lyophilized and then dissolved in 0.5 mL of D_2O (99.8%); this procedure was repeated one more time, and the samples were equilibrated for at least 4 days at 23 °C to ensure complete exchange of labile protons.

Electrochemistry. Midpoint redox potentials were determined at room temperature by differential pulse voltammetry using a BAS CV-50W voltammetric analyzer or by anaerobic spectrophotometric redox titrations. Titrations were carried out in 1.0 mL quartz spectrochemical cells (1.0 cm path length) containing 0.1 mM ferredoxin and 10 μM methyl viologen (−430 mV vs NHE) or benzyl viologen (−350 mV) as mediators in 20 mM Tris-HCl, pH 8.0, and 100 mM NaCl. The samples were titrated with 0.1 M sodium dithionite in an anaerobic chamber. The ambient potential of the solution after each aliquot was measured using a Beckman DM15B voltmeter fitted with a platinum electrode and a calomel reference electrode, and spectra were recorded. For the calculation of the midpoint potential, the absorbances of the ferredoxin samples were determined at 422 nm ($\Delta\epsilon$ ~4700 M^{-1} cm^{-1}), a wavelength where the mediators undergo little absorbance change (Batie & Kamin, 1981). Plots of the absorbance vs potential data were fit to the Nernst equation for a single electron transfer process by nonlinear least square regression analysis to acquire values for the midpoint potentials and the limiting absorbances. The obtained values for the limiting absorbances were used to calculate the percentage of reduction of each sample at each point of the titration curve.

Kinetic Studies. The reduced form of the ferredoxin was generated by addition of 1−2 equiv of sodium dithionite in degassed solution to a deoxygenated ferredoxin solution at the required pH and ionic strength under anaerobic conditions. The reduced form was used within 1 h of addition of dithionite. Kinetic measurements were carried out using an OLIS stopped-flow spectrophotometer. Reaction progress was followed by monitoring the increase in absorbance of the solution at 422 nm. All reactions were carried out under pseudo-first-order conditions with oxidant in at least 8-fold excess. A nonlinear least squares program was used to fit data to single exponential rate laws, with satisfactory fits reflected by values for Durbin−Watson factors greater than 1.8. The rate constants reported were an average of at least four stopped-flow traces for the same reactant solution.

With the oxidant in large excess, the kinetics of the reaction of the reduced ferredoxin with oxidants conform to rate law 1:

$$\text{rate} = k_{obs}[Fe_2S_2(SR)_4^{3-}] \quad (1)$$

A nonlinear dependence of k_{obs} on concentration of oxidants is observed for the reaction of [2Fe-2S] ferredoxins with $Co(NH_3)_6^{3+}$. Observed rate dependence on oxidant concentration is consistent with a two-step mechanism involving association (eq 2) followed by electron transfer (eq 3)

$$Fe_2S_2(SR)_4^{3-} + L_6Co^{III} \underset{k_{-1}}{\overset{k_1}{\rightleftharpoons}} Fe_2S_2(SR)_4^{3-} - L_6Co^{III} \quad (2)$$

$$Fe_2S_2(SR)_4^{3-} - L_6Co^{III} \xrightarrow{k_{et}} Fe_2S_2(SR)_4^{2-} + L_6Co^{II} \quad (3)$$

With the low-spin Co(III) complexes used in this study, the intramolecular rate constant k_{et} is small relative to k_1 and k_{-1}; resultantly, the rate law governing the appearance of products may be simplified by a steady state approximation for the concentration of the Fe(II, III) Co(III) complex. In this event, the overall rate law reduces to eq 4:

$$k_{obs} = \frac{Kk_{et}[L_6Co^{III}]}{1 + K[L_6Co^{III}]} \quad (4)$$

where K is the association constant and k_{et} is the intramolecular ET rate constant. Values of K and k_{et} were obtained iteratively by nonlinear regression fits of the data to eq 4 (1% allowable error).

RESULTS

The first objective of the study was to devise a procedure for expression of the vegetative *Anabaena* ferredoxin gene in *E. coli*. To this end, an expression system based on the T7 RNA polymerase promoter was chosen due to its well-known efficacy to produce substantial yields of recombinant proteins (Studier et al., 1990). Expression of the WT ferredoxin gene using this protocol proceeded efficiently, affording over 20 mg of pure protein per liter of culture. The Ala45Ser mutant was obtained in a similar yield. An important feature of this protocol is the direct isolation of the holoprotein from the bacterial cells. Previous reports of expression of *Anabaena* ferredoxins in *E. coli* did not report yields (Bohme & Haselkorn, 1989) or required an additional denaturation−renaturation protocol to obtain the holoprotein from cell lysate (Hurley et al., 1993; Cheng et al., 1994) in yields of 2−20 mg per liter.

The recombinant WT protein displayed biochemical properties identical to those of authentic ferredoxin (Bohme & Schrautemeier, 1987a). On native polyacrylamide gels (12%), recombinant ferredoxin could be seen as an orange band that ran close to the bromphenol blue marker, as did the authentic protein. Electrophoresis of the WT ferredoxin on SDS−PAGE gels resulted in a diffuse band at an apparent molecular mass of 23−27 kDa. Isoelectric focusing revealed the purified recombinant protein to have an isoelectric point of 2.8 which agreed with the pI value of 2.6 for the protein isolated from *Anabaena* cells (Bohme & Schrautemeier, 1987a). The electrophoretic properties of the Ala45Ser variant were indistinguishable from those of the WT.

The UV−vis spectrum of the recombinant WT protein was identical to that of the protein isolated from natural sources (Bohme & Schrautemeier, 1987a), with bands at 276, 330, 422, and 464 nm (Figure 1). Likewise, the CD spectrum of the expressed protein was identical to that of the cyanobacterial ferredoxin, displaying positive extrema at 361 and 437 nm and negative extrema at 384, 510, and 562 nm (Figure 2).

Although differences between the UV−vis spectra of Ala45Ser and WT ferredoxin were not discernible (Figure

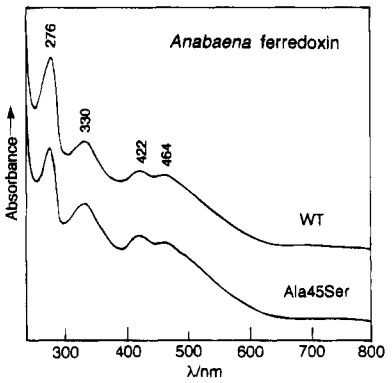

FIGURE 1: UV−vis spectra of WT *Anabaena* ferredoxin (top) and the Ala45Ser mutant (bottom) in 20 mM Tris-HCl, pH 8.0, and 100 mM NaCl.

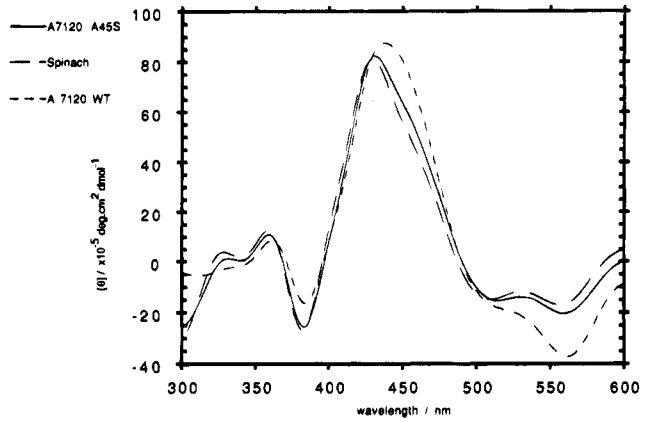

FIGURE 2: CD spectra of WT *Anabaena* ferredoxin, the Ala45Ser mutant, and spinach ferredoxin in 20 mM Tris-HCl, pH 8.0, and 100 mM NaCl.

1), differences were apparent in the CD spectra (Figure 2). In particular, the negative band at 560 nm in the spectrum of the mutant protein was significantly less intense than the analogous band of the WT protein, the band at 431 nm in the mutant spectrum was narrower than the band at 437 nm in the WT spectrum, and positive and negative bands at 331 and 280 nm, respectively, were present in the spectrum of the mutant protein, which were not seen in the WT spectrum. Interestingly, the CD spectral characteristics of Ala45Ser *Anabaena* ferredoxin were essentially indistinguishable from those of spinach ferredoxin, a typical higher plant ferredoxin which also has a serine residue at position 45.

The X-band EPR spectra of sodium dithionite-reduced WT and Ala45Ser *Anabaena* ferredoxins were also recorded. The EPR spectrum of the reduced proteins displayed features characteristic of rhombic symmetry that were typical of photosynthetic ferredoxins (Figure 3). Accurate values for the principal g factors were obtained through computer simulation of the spectra. Broadening of lines in EPR spectra of [2Fe-2S] ferredoxins as a result of g strain is well-documented (Hagen, 1992), and faithful simulated representations are possible only by considering anisotropic line width terms. The spectrum of the Ala45Ser mutant was distinct from that of the WT protein, as reflected by differences in the line widths and values of the g factors (Table 1). Interestingly, the values of the g factors of the Ala45Ser variant were similar to those of spinach ferredoxin (Ohmori et al., 1989).

Further notable differences in the spectroscopic properties of the WT and Ala45Ser proteins were discernible in the

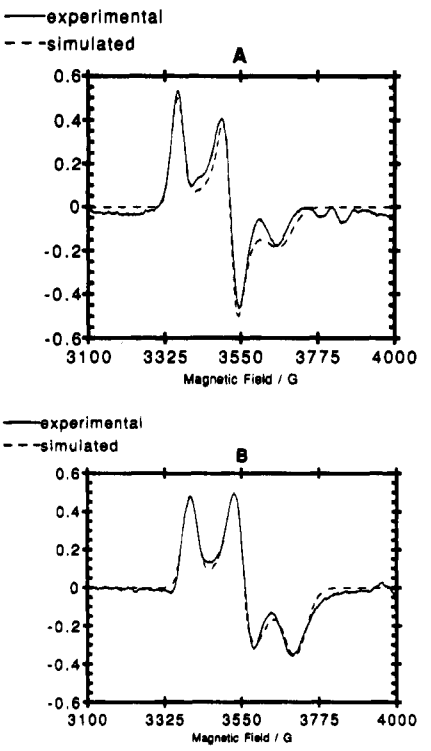

FIGURE 3: X-band EPR spectra (10 K) of (A) WT and (B) Ala45Ser *Anabaena* ferredoxins, recorded at 9.72 and 9.79 GHz, respectively. The features at 3420 and 3780 G are due to an impurity. Experimental spectra are shown as solid lines, and simulated spectra are shown as dashed lines. Simulation parameters for spectrum A were $g_x = 1.893$, $g_y = 1.973$, $g_z = 2.067$, $W_x = 26.88$ G, $W_y = 22.01$ G, and $W_z = 21.41$ G and for spectrum B were $g_x = 1.902$, $g_y = 1.954$, $g_z = 2.044$, $W_x = 43.14$ G, $W_y = 28.68$ G, $W_z = 22.14$ G, $W_{xy} = -8.6$ G, $W_{xz} = 16.0$ G, and $W_{yz} = 1.14$ G, where W_n and W_{mn} are the residual line width and off-diagonal line width terms, respectively.

Table 1: EPR Spectra Parameters of [2Fe-2S] Ferredoxins

		EPR[a]				
protein class	source	g_x	g_y	g_z	δ/ζ	R
cyanobacterial	*A.* 7120[b]	1.893	1.973	2.067	22.6	92
	N. MAC I[c]	1.885	1.960	2.053	22.2	83
	S. maxima[d]	1.884	1.950	2.044	22.5	80
higher plant	*S. oleracea* I[e]	1.890	1.95	2.04	23.9	75
	P. sativum[c]	1.90	1.96	2.03	29.3	70
	A. 7120 Ala45Ser[b]	1.902	1.954	2.044	24.3	65

[a] X-band EPR spectra obtained at 10 K. Parameters δ/ζ and R calculated according to Blumberg and Peisach (1974) $\{\delta/\zeta = 4/3[1/(g_z - g_x) + 1/(g_z - g_y)]$; $R = 300[(g_y - g_x)/(2g_z - g_y - g_x)]\}$. [b] g values were obtained by spectral simulation. *A.* 7120: *Anabaena* PCC7120. [c] *N.* is *Nostoc.* Hutson et al. (1978). [d] Blumberg and Peisach (1974). [e] Ohmori et al. (1989a).

resonance Raman (RR) spectra of the proteins (Figures 4 and 5). RR spectra of [2Fe-2S] clusters show a number of peaks between 250 and 450 cm^{-1} due to modes associated with Fe−S stretching vibrations, which are enhanced via S → Fe charge transfer (CT) transitions (Han et al., 1989b). On the basis of extensive IR and RR studies of isotopically labeled synthetic model compounds, reliable vibrational assignments for the various bands are available (Han et al., 1989b).

The previously unreported RR spectrum of WT *Anabaena* ferredoxin, obtained with 458 nm laser excitation, is shown in Figure 4. The intensities and frequencies of the bands of

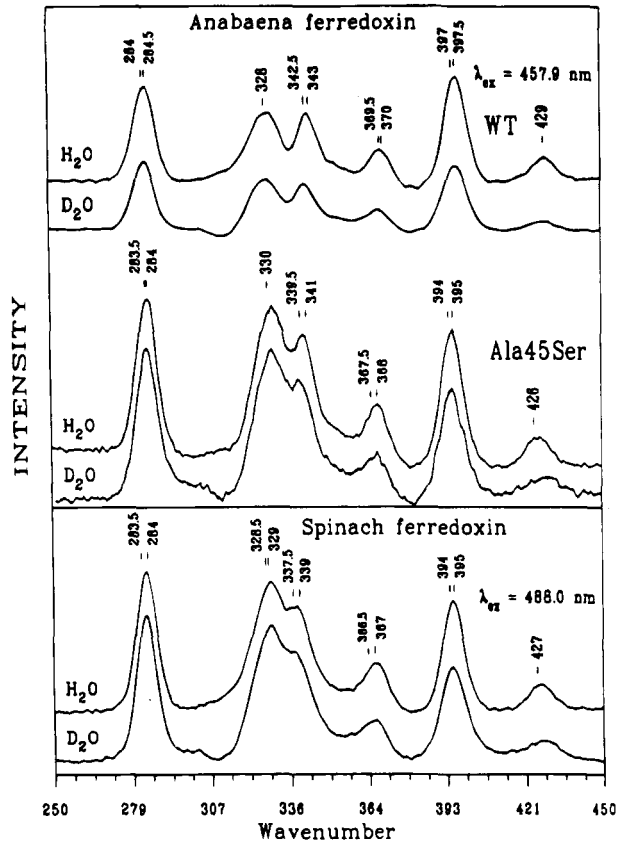

FIGURE 4: Resonance Raman spectra of WT *Anabaena* ferredoxin (top), Ala45Ser ferredoxin (middle), and spinach ferredoxin (bottom) obtained using 458 nm excitation. Spectra recorded in D_2O are the bottom and spectra recorded in H_2O the top of the pairs.

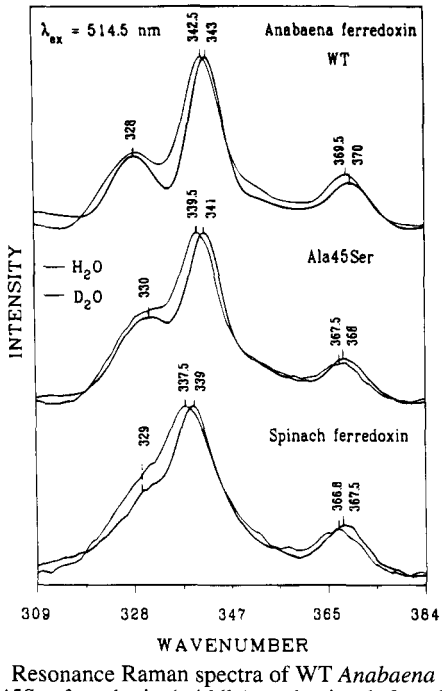

FIGURE 5: Resonance Raman spectra of WT *Anabaena* ferredoxin (top), Ala45Ser ferredoxin (middle), and spinach ferredoxin (bottom) obtained using 514 nm excitation. Spectra recorded in D_2O are the bottom and spectra recorded in H_2O the top of the pairs.

the *Anabaena* protein spectrum show similarities to those for other cyanobacterial ferredoxins, such as *Spirulina platensis* ferredoxin (Mino et al., 1987) (Table 2). Spectra were also obtained with 514 nm excitation to complement the 458 nm excitation data since the former display more significant enhancements of the terminal Fe−S stretching vibrational modes (Figure 5).

In the RR spectrum of Ala45Ser *Anabaena* ferredoxin, the A_g^t terminal Fe−S stretching peak downshifts to 341 cm^{-1} (−2 cm^{-1}) and the B_{3u}^b, A_g^b, and B_{2u}^b bridging Fe−S stretching peaks downshift to 368 (−2), 395 (−2.5), and 426 (−3) cm^{-1}, respectively, relative to the WT spectrum (Figure 4). Additionally, the intensity of the A_g^t peak decreases significantly relative to the analogous band in the WT spectrum. Spinach ferredoxin displays a RR spectrum with an identical pattern of peak intensities and similar energies as Ala45Ser *Anabaena* ferredoxin (Table 2 and Figure 4).

When samples of iron−sulfur proteins are equilibrated with D_2O, isotope dependent shifts are often detected in RR spectra (Mino et al., 1987). Deuterated samples of WT and Ala45Ser *Anabaena* ferredoxin displayed different extents of shifts in RR peaks (Figures 3 and 4, Table 2). In the WT spectrum, the A_g^t band downshifts to 342.5 cm^{-1} (−0.5 cm^{-1}) and the B_{3u}^b peak downshifts to 369.5 cm^{-1} (−0.5 cm^{-1}). In the spectrum of the Ala45Ser variant, the A_g^t peak downshifts more substantially to 339.5 cm^{-1} (−1.5 cm^{-1}) and the B_{3u}^b peak downshifts to 367.5 cm^{-1} (−0.5 cm^{-1}). Deuterium dependent shifts are also discernible in the 488 nm-excited spectrum of spinach ferredoxin (Figure 4); the pattern of shifts was identical to the pattern seen for the Ala45Ser *Anabaena* mutant (Table 2).

Midpoint redox potentials for the WT and mutant ferredoxins were measured by spectrophotometric redox titrations (Figure 6). The redox potential for WT *Anabaena* 7120 ferredoxin was detremined to be −406 ± 10 mV vs NHE, somewhat higher than the value obtained by other workers for the same protein using potentiometric techniques (−449 mV, Salamon & Tollin, 1992). The value for the Ala45Ser mutant obtained by the spectrophotometric redox titration method was −382 ± 10 mV. Reversible electron transfer behavior was observed for both the mutant and WT *Anabaena* 7120 proteins at a gold electrode modified with a polymeric methyl viologen monolayer (Landrum et al., 1977). The values for the redox potentials obtained by DPV using the modified gold electrode were −439 mV (WT) and −420 mV (Ala45Ser), somewhat lower than those obtained by the titration method.

The kinetics of the electron transfer reaction of the dithionite-reduced ferredoxins with select cobalt complexes were measured by stopped-flow spectrometry. Under the reaction conditions, the kinetic behavior of the species could be accurately represented by a mechanism involving preassociation of the negatively charged protein and positively charged inorganic reagent, followed by electron transfer to generate the reduced cobalt complex and the oxidized protein (see Experimental Procedures). The values for the bimolecular association (K) and electron transfer rate (k_{et}) parameters for reaction with $Co(NH_3)_6^{3+}$ of WT and Ala45Ser *Anabaena* ferredoxins as well as those of typical cyanobacterial (*S. platensis*) and chloroplast (parsley) ferredoxins are shown in Table 3.

DISCUSSION

Previously published methods for expressing *Anabaena* ferredoxins in *E. coli* provided either the holoproteins in moderate yield or apoproteins, which were reconstituted with iron and inorganic sulfide *in vitro* (Bohme & Haselkorn, 1989; Hurley et al., 1993; Cheng et al., 1994). The method

Table 2: Frequencies and Assignments of Bands in RR Spectra of [2Fe-2S] Ferredoxins[a]

protein source	$B_{3u}{}^t$	$B_{1g}{}^b$	$A_g{}^t$	$B_{3u}{}^b$	$A_g{}^b$	$B_{2u}{}^b$
A. 7120 WT	284.5 (−0.5)	328 (0)	343 (−0.5)	370 (−0.5)	397.5 (−0.5)	429
S. platensis[b]	283 (−0.2)	328 (−0.5)	340 (−0.5)	367 (−0.6)	394 (−0.2)	425
A. 7120 Ala45Ser	284 (−0.5)	330 (0)	341 (−1.5)	368 (−0.5)	395 (−1.0)	426
S. oleracea	284 (−0.5)	329 (−0.5)	339 (−1.5)	367 (−0.5)	395 (−1.0)	427

[a] Frequencies in cm^{-1}; deuterium dependent shifts in parentheses given as frequency in H_2O minus frequency in D_2O. Spectral conditions as in Figures 3 and 4. Peak positions determined by curve fitting. Assignments from Han et al. (1989a). *A.* 7120: *Anabaena* PCC7120. [b] Mino et al. (1987).

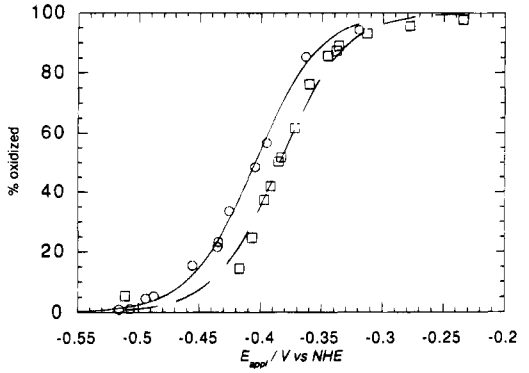

FIGURE 6: Spectrophotometric reductive titration of WT (○) and Ala45Ser (□) ferredoxins with dithionite at room temperature. Absorption change was monitored at 422 nm. The solid lines are theoretical plots of the Nernst equation for a one-electron carrier with midpoint potentials of −406 mV (WT) and −382 mV (Ala45Ser) vs NHE.

Table 3: Values of Association Constants (K) and Intracomplex Electron Transfer Rate Constants (k_{et}) for the Reaction of Select [2Fe-2S] Ferredoxins with $Co(NH_3)_6^{3+}$ [a]

source	K (M^{-1})	k_{et} (s^{-1})
A. 7120 WT[b]	2080 (152)	2.74 (0.08)
S. platensis[c]	2070	4.9
A. 7120 Ala45Ser[b]	1840	2.95 (0.10)
parsley[d]	917 (97)	19.5 (0.7)

[a] 10 mM Tris-HCl, pH 8.0, and 0.1 M NaCl. Standard deviations are shown in parentheses. [b] *A.* 7120: *Anabaena* PCC7120. [c] Adzamli et al. (1983). [d] Armstrong and Sykes (1978).

described afforded *Anabaena* ferredoxin as the holoprotein in high yield (over 20 mg per liter) and thus represents the procedure of choice for obtaining this protein and its mutants. On electrophoresis, the recombinant ferredoxin was indistinguishable from the protein isolated from *Anabaena* sp. 7120 cells. The electrophoretic behavior of Ala45Ser ferredoxin was identical to that of the WT protein, indicating that the mutation had minimal effect on the electrostatic properties of the protein.

Proteins containing [2Fe-2S] clusters display complex absorption spectra, which originate from a number of overlapping S → Fe(III) CT transitions. The UV−vis spectra of the WT and Ala45Ser ferredoxins display identical absorption maxima and intensities (Figure 1). Because the absorption spectra of most photosynthetic ferredoxins are indistinguishable from each other, the fact that the spectra of the WT and Ala45Ser proteins are alike was not unexpected. The CT transitions are better resolved in the CD spectra of [2Fe-2S] ferredoxins, and differences are discernible between cyanobacterial and higher plant ferredoxins (Stephens et al., 1978; Ohmori et al., 1989). The CD spectral properties of *Anabaena* Ala45Ser ferredoxin were distinct from those of the WT protein and were essentially identical to those of spinach ferredoxin, which has a Ser residue at position 45. Although the identities of the CT transitions that give rise to the various bands in the CD spectra of oxidized [2Fe-2S] proteins have not been been definitively assigned, terminal S → Fe(III) CT bands have been shown to appear around 520 nm based on RR excitation profiles (Mino et al., 1989). Interestingly, the most prominent difference in the CD spectra of the mutant and WT ferredoxins is observed in this region.

EPR spectroscopy has been shown to be of great value in the characterization of the properties of reduced [2Fe-2S] clusters in proteins (Hagen, 1992). Mossbauer studies of reduced ferredoxins have demonstrated that the metal cluster exists in a "valence-trapped" state, which contains one formal Fe(III) ion and one formal Fe(II) ion (Gibson et al., 1966). In photosynthetic ferredoxins, the formal Fe(II) ion has been shown to be the one ligated to Cys 41 and Cys 46 (Dugad et al., 1990). Antiferromagnetic coupling of the iron atoms in reduced ferredoxins gives rise to a characteristic EPR spectrum with a g_{av} value lower than that of the free electron ($g = 2.0022$).

Blumberg and Peisach have devised a method to interpret the EPR-derived g values of [2Fe-2S] clusters in terms of parameters that measure the symmetry and the extent of covalency at the Fe(II) site (Blumberg & Peisach, 1974). These parameters, δ/ζ and R, measure the protein dependent spin delocalization and geometric arrangement, respectively, at the reduced iron atom. The δ/ζ parameter affords a measure of the degree of covalent interaction between the reduced metal site and the protein surroundings; higher values of δ/ζ signify increasing covalency at the ferrous site. The parameter R, or percent rhombicity, reflects the degree of rhombicity, i.e. symmetry, at the ferrous site. The δ/ζ and percent rhombicity values for WT and Ala45Ser *Anabaena* ferredoxins are shown in Table 1. The mutant cluster has higher symmetry at the reduced iron site relative to the WT cluster and also displays increased covalency at the reducible iron center relative to the WT. For comparison, the R and δ/ζ quantities are also shown for other ferredoxins; the values for these parameters for the Ala45Ser mutant are more similar in magnitude to those for higher plant than for cyanobacterial ferredoxins.

RR spectroscopy has been extensively utilized to investigate the characteristics of [2Fe-2S] clusters in proteins, due to its sensitivity to differences in electronic and geometric features. Through a combination of infrared and RR analysis of isotopically labeled model compounds and normal mode calculations, the vibrational modes that give rise to the peaks in the spectra of [2Fe-2S] clusters in proteins have been identified (Han et al., 1989a). The RR spectra of many [2Fe-2S] proteins have been reported (Mino et al., 1987; Han et al., 1989b; Fu et al., 1992), in both the reduced and oxidized states; the variation in the appearance of the spectra reflects the variation in ground and excited state structures of the

entire clusters (oxidized state) or of the localized ferric site (reduced state).

The RR spectra of *Anabaena* sp. 7120 ferredoxin are shown in Figures 4 and 5. The overall appearance of the WT spectrum, including peak frequencies and intensities, is very similar to that of other cyanobacterial ferredoxins, such as *S. platensis* (Mino et al., 1987). The spectrum of Ala45Ser ferredoxin, however, has a different appearance and is actually more similar to that of spinach ferredoxin (Figure 4) than to that of WT *Anabaena* ferredoxin. Likewise, the pattern of deuterium specific shifts of the RR bands of the variant ferredoxin more closely resembles the pattern for spinach ferredoxin than that for the WT *Anabaena* protein.

The most evident difference between the RR spectra of the WT and Ala45Ser ferredoxins is in the appearance of the A_g^t peak near 340 cm^{-1} (Figures 4 and 5). This band is assigned to stretching motions of the terminal iron−sulfur bonds (Han et al., 1989a). The intensity of the A_g^t peak is diminished in both the Ala45Ser and spinach ferredoxin spectra relative to the WT *Anabeana* spectrum. In addition, this peak experiences more significant deuterium shifts in the former two proteins' spectra. Both relatively weak intensities and large deuterium shifts of peaks in metalloprotein RR spectra are indicative of the presence of hydrogen-bonding interactions from the protein matrix to ligand atoms of the metal center (Mino et al., 1987; Fu et al., 1992). Thus, the RR spectroscopic data indicate that the terminal sulfur atoms of the [2Fe-2S] clusters in both the Ala45Ser *Anabaena* and spinach ferredoxins experience a greater degree of hydrogen-bonding interactions from protein donor atoms relative to those of WT *Anabaena* ferredoxin. These results are consistent with the EPR investigations that concluded that the reducible iron site of the Ala45Ser and spinach ferredoxin clusters was involved in greater covalent interactions with the protein surroundings that the redox active iron of WT *Anabaena* ferredoxin.

Functionally, substitution of Ser for Ala at position 45 of *Anabaena* ferredoxin results in a protein with kinetic characteristics in the reaction with $Co(NH_3)_6^{3+}$ that approach those of ferredoxins from higher plants. In other words, the value of K for the mutant is substantially lower while the value for k_{et} is higher than the corresponding values for the WT. It is clear that, while not completely responsible for determining the ET characteristics of photosynthetic ferredoxins, the residue at position 45 affects the reactivity of the iron−sulfur cluster with the positively charged cobalt complex. A reasonable explanation for these results is that the serine side chain more effectively shields the anionic ligands from interaction with the positively charged reagent, lowering the association and ET rate constants through increased steric hindrance.

The anionic character of the sulfur ligands in iron−sulfur proteins makes them strong hydrogen bond acceptors. X-ray structural investigations of several [2Fe-2S] ferredoxins have revealed that a number of backbone amide groups are positioned sufficiently close (3.3−3.4 Å) to both terminal and bridging sulfur atoms of the cluster to form hydrogen bonds (Fukuyama et al., 1981; Rypniewski et al., 1991). Recent pulsed ENDOR studies of [2Fe-2S] ferredoxins (Fan et al., 1992) and NMR investigations of the simple iron−sulfur protein rubredoxin (Blake et al., 1992) have provided evidence of electron spin density on specific amide hydrogen atoms of the peptide backbone. Spectroscopic studies of various model iron−sulfur complexes have also supported the existence of NH to sulfur hydrogen bonds (Ueyama et al., 1992).

An attractive rationalization for the additional protein-terminal sulfur ligand hydrogen-bonding interactions observed in ferredoxins with Ser at position 45 relative to proteins with Ala at the same position would be the presence of a hydrogen bond from the side chain hydroxyl of Ser 45 to a specific cysteinyl sulfur ligand. Inspection of the structure of WT *Anabaena* ferredoxin (Rypniewski et al., 1991) reveals that the methyl group of Ala 45 is located on the surface of the protein in close proximity to the ligand sulfur atom of Cys 41. According to the crystal structure of vegetative *Anabaena* ferredoxin, Holden and co-workers state that the sulfur atom of Cys 41 is within hydrogen-bonding distance of two backbone amide hydrogens, those of Ala 43 and Ala 45 (Rypniewski et al., 1991); close inspection of the structure reveals, however, that the amide hydrogen atom of Ala 45 is not directed to a sulfur lone pair orbital, but rather directly between the two orbitals, and is therefore geometrically unfavorable. The conjecture that this hydrogen bond is insignificant is supported by the small deuterium shifts of the terminal Fe−S stretching vibrations in the RR spectrum of WT *Anabaena* ferredoxin. On the basis of a computer model of the Ala45Ser mutant, the Ser 45 hydroxyl group would locate itself 3.4 Å from the sulfur atom of Cys 41 and would form a geometrically ideal hydrogen bond to the *pro-R* sulfur lone pair. Other support for the existence of OH to S hydrogen bonds in iron−sulfur proteins comes from high-resolution crystal structures of cyanobacterial [2Fe-2S] ferredoxins, which show that the side chain hydroxyl groups of Ser 40 and Thr 48 are capable of forming geometrically favorable hydrogen bonds to the sulfur atom of Cys 46 (3.4 Å S to N distance) (Fukuyama et al., 1981; Rypniewski et al., 1991).

Hydrogen-bonding interactions between ligand atoms and side chain and main chain donor atoms have been proposed to modulate oxidation−reduction potentials of metal ions in proteins. For example, the bacterial [4Fe-4S] ferredoxins cycle between the $[Fe_4S_4(Cys)_4]^{2-/3-}$ oxidation states at potentials in the range of −250 to −600 mV (Lovenberg, 1973). The high-potential iron proteins (HIPIP's), on the other hand, cycle between $[Fe_4S_4(Cys)_4]^{1-/2-}$ states at potentials between +50 and +450 mV, with potentials for the $[Fe_4S_4(Cys)_4]^{2-/3-}$ interconversion considerably lower than −600 mV (Meyer et al., 1983). Crystallographic and RR studies of these proteins have revealed a greater number of amide−sulfur hydrogen bonds in the ferredoxins than in the HIPIP's (Backes et al., 1991). The additional hydrogen bonds in the bacterial ferredoxins presumably stabilize the $[Fe_4S_4(Cys)_4]^{3-}$ state relative to the HIPIP's. In this regard, it is important to note that the midpoint potential of Ala45Ser *Anabaena* ferredoxin is appreciably higher (−382 mV) than the potential of WT *Anabaena* ferredoxin (−406 mV); the effect of an additional, geometrically favorable hydrogen bond from the Ser 45 hydroxyl group to the sulfur atom of Cys 41 (a ligand of the reducible iron center) on redox potentials in [2Fe-2S] ferredoxins would be consistent with the relationship between the number of hydrogen bonds and redox potentials in [4Fe-4S] proteins. Since the values for the redox potentials for most plant ferredoxins (below −400 mV, Stombaugh et al., 1972) are lower than those for

cyanobacterial proteins (−305 to −380 mV), the presence of the serine residue at position 45 cannot be the primary determinant of the lower potentials of the plant ferredoxins, and variations at other positions of the primary sequence must be responsible.

CONCLUSIONS

1. The identity of the residue at position 45 on the metal-binding loop of photosynthetic [2Fe-2S] ferredoxins controls the appearance of the spectra (CD, EPR, and RR), allowing the distinction between those proteins with Ala and those with Ser at position 45.

2. The spectrochemical properties support the presence of a Ser 45 (OH) to Cys 41 (S) hydrogen bond in Ala45Ser *Anabaena* and spinach ferredoxins.

3. The presence of an additional Ser OH to ligand S hydrogen bond in Ala45Ser ferredoxin relative to WT *Anabaena* ferredoxin is responsible for the higher midpoint potential of the mutant ferredoxin relative to the WT protein.

ACKNOWLEDGMENT

The authors express their gratitude to Mr. V. Kurchev for assistance in obtaining the EPR spectra, Mr. C. Segler and Mr. H. Wang for protein preparation, and Prof. S. E. Curtis of the Department of Genetics, North Carolina State Univeristy, for the plasmid pAn662.

SUPPORTING INFORMATION AVAILABLE

Saturation kinetics plots for oxidation of ferredoxin by $Co(NH_3)_6^{3+}$ (2 pages). Ordering information is given on any current masthead page.

REFERENCES

Adzamli, I. K., Petrou, A., Sykes, A. G., Rao, K. K., & Hall, D. O. (1983) *Biochem. J. 211*, 219−226.

Alam, J., Whittaker, R. A., Krogmann, D. W., & Curtis, S. E. (1986) *J. Bacteriol. 168*, 1265−1271.

Armstrong, F. A., & Sykes, A. G. (1978) *J. Am. Chem. Soc. 110*, 7710−7715.

Backes, G., Mino, Y., Loehr, T. M., Meyer, T. E., Cusanovich, M. A., Sweeney, W. V., Adman, E. T., & Sanders-Loehr, J. (1991) *J. Am. Chem. Soc. 113*, 2055−2064.

Batie, C. J., & Kamin, H. (1981) *J. Biol. Chem. 256*, 7756−7763.

Blake, P. R., Park, J. B., Adams, M. W. W., & Summers, M. F. (1992) *J. Am. Chem. Soc. 114*, 4931−4933.

Blumberg, W. E., & Peisach, J. (1974) *Arch. Biochem. Biophys. 162*, 502−512.

Bohme, H., & Haselkorn, R. (1989) *Plant Mol. Biol. 12*, 667−672.

Bohme, H., & Schrautemeier, B. (1987a) *Biochim. Biophys. Acta 891*, 1−7.

Bohme, H., & Schrautemeier, B. (1987b) *Biochim. Biophys. Acta 891*, 115−120.

Cammack, R., Krishna Rao, K., Bargeron, C. P., Hutson, K. G., Andrew, P. W., & Rogers, L. J. (1977) *Biochem. J. 168*, 205−209.

Cheng, H., Xia, B., Reed, G. H., & Markley, J. L. (1994) *Biochemistry 33*, 3155−3164.

Czernuszewicz, R. S. (1993) in *Methods in Molecular Biology* (Jones, C., Mulloy, B., & Thomas, A. H., Eds.) pp 345−374, Humana Press, Totawa, NY.

Dugad, L. B., Le Mar, G. N., Banci, L., & Bertini, I. (1990) *Biochemistry 29*, 2263−2271.

Fan, C., Kennedy, M. C., Beinert, H., & Hoffman, B. M. (1992) *J. Am. Chem. Soc. 114*, 374−375.

Fu, W., Drozdzewski, P. M., Davies, M. D., Sligar, S. G., & Johnson, M. K. (1992) *J. Biol. Chem. 267*, 15502−15510.

Fukuyama, K., Hase, T., Matsumoto, S., Tsukihara, T., Katsube, Y., Tanaka, N., Kakudo, M., Wada, K., & Matsubara, H. (1980) *Nature 286*, 522−524.

Fukuyama, K., Hase, T., Matsumoto, S., Tsukihara, T., Katsube, Y., Tanaka, N., Kakudo, M., Wada, K., & Matsubara, H. (1981) *J. Biochem. 90*, 1763−1773.

Gibson, J. F., Hall, D. O., Thornley, J. H. M., & Whatley, F. R. (1966) *Proc. Natl. Acad. Sci. U.S.A. 56*, 987−990.

Guo, L.-H., & Hill, H. A. O. (1991) in *Advances in Inorganic Chemistry* (Sykes, A. G., Ed.) Vol. 36, pp 341−376, Academic Press, New York.

Hagen, W. R. (1992) in *Advances in Inorganic Chem*istry (Cammack, R., & Sykes, A. G., Eds.) Vol. 38, pp 165−222, Academic Press, New York.

Han, S., Czernuszewicz, R. S., & Spiro, T. G. (1989a) *J. Am. Chem. Soc. 111*, 3496−3504.

Han, S., Czernuszewicz, R. S., Kimura, T., Adams, M. W. W., & Spiro, T. G. (1989b) *J. Am. Chem. Soc. 111*, 3505−3511.

Holden, H. M., Jacobsen, B. L., Hurley, J. K., Tollin, G., Oh, B.-H., Skjeldal, L., Chae, Y. K., Cheng, H., Xia, B., & Markley, J. L. (1994) *J. Bioenerg. Biomembr. 26*, 67−88.

Hurley, J. K., Salamon, Z., Meyer, T. E., Fitch, J. C., Cusanovich, M. A., Markley, J. L., Cheng, H., Xia, B., Chae, Y. K., Medina, M., Gomez-Moreno, C., & Tollin, G. (1993) *Biochemistry 32*, 9346−9354.

Hutson, K. G., Rogers, L. J., Haslett, B. G., Boulter, D., & Cammack, R. (1978) *Biochem. J. 172*, 465−477.

Jacobsen, B. L., Chae, Y. K., Markley, J. L., Rayment, I., & Holden, H. M. (1993) *Biochemistry 32*, 6788−6793.

Knaff, D. B., & Hirasawa, M. (1991) *Biochim. Biophys. Acta 1056*, 93−125.

Kunkel, T. A., Roberts, J. D., & Zakour, R. A. (1987) *Methods Enzymol. 154*, 267−382.

Landrum, H. L., Salmon, R. T., & Hawkridge, F. M. (1977) *J. Am. Chem. Soc. 99*, 3154−3158.

Lovenberg, W., Ed. (1973) *Iron-Sulfur Proteins*, Vols. I and II, Academic Press, New York.

Maniatis, T., Fritsch, F. F., & Sambrook (1989) *Molecular Cloning: A Laboratory Manual*, 2nd ed., CSH Laboratory Press, Cold Spring Harbor.

Matsubara, H., & Hase, T. (1983) in *Proteins and Nucleic Acids in Plant Systematics* (Jensen, U., & Fairbrothers, D. E., Eds.) pp 168−181, Springer-Verlag, New York.

Matsubara, H., & Saeki, K. (1991) in *Advances in Inorganic Chem*istry (Cammack, R., Ed.) Vol. 38, pp 223−267, Academic Press, New York.

Meyer, T. E., Przysiecki, C. T., Watkins, J. A., Bhattacharyya, A., Simondsen, R. P., Cusanovich, M. A., & Tollin, G. (1983) *Proc. Natl. Acad. Sci. U.S.A. 80*, 6740−6744.

Mino, Y., Loehr, T. L., Wada, K., Matsubara, H., & Sanders-Loehr, J. (1987) *Biochemistry 26*, 8059−8065.

Oh, B.-H., & Markley, J. L. (1990) *Biochemistry 29*, 3993−4004.

Oh, B.-H., Mooberry, E. S., & Markley, J. L. (1990) *Biochemistry 29*, 4004−4011.

Ohmori, D., Hasumi, H., Yamakura, F., Murakami, M., Fujisawa, K., Taneoka, Y., & Yamamura, T. (1989) *Biochim. Biophys. Acta 996*, 166−172.

Rao, K. K., Cammack, R., Hall, D. O., & Johnson, C. E. (1971) *Biochem. J. 122*, 257−265.

Rogers, L. (1987) in *The Cyanobacteria* (Fay, P., & van Balen, C., Eds.) pp 35−67, Elsevier, New York.

Rypniewski, W. R., Breiter, D. R., Benning, M. M., Wesenberg, G., Oh, B. H., Markley, J. L., Ryment, I., & Holden, H. M. (1991) *Biochemistry 30*, 4126−4131.

Stephens, P. J., Thomson, A. J., Dun, J. B. R., Keiderling, T. A., Rawlings, J., Rao, K. K., & Hall, D. G. (1978) *Biochemistry 17*, 4770−4778.

Stombaugh, N. A., Sundquist, J. E., Burris, R. H., & Orme-Johnson, W. H. (1976) *Biochemistry 15*, 2633−2640.

Studier, F., Rosenberg, A. H., & Dunn, J. J. (1990) *Methods Enzymol. 185*, 60−89.

Tsukihara, T., Fukuyama, K., Mizushima, M., Harioka, T., Kusunoki, M., Katsube, Y., Hase, T., & Matsubara, H. (1990) *J. Mol. Biol. 216*, 399−410.

Ueyama, N., Okamura, T., & Nakamura, A. (1992) *J. Chem. Soc., Chem. Commun.*, 1019−1020.

BI951256Y